AIAA SciTech Forum
8–12 January 2018, Kissimmee, Florida
2018 Wind Energy Symposium

10.2514/6.2018-1244

Measurements of Wind Turbine Tower Shadow and Fairing Effects

Carlos Noyes[1], Chao Qin[2] and Eric Loth[3]
University of Virginia, Charlottesville, VA, 22904

ABSTRACT

Downwind two-bladed rotor configuration can have advantages in reducing rotor mass for wind turbines, compared with three-bladed upwind design. However, the tower shadow adds an aerodynamic complication that can be difficult to quantify and predict. This study presents and analyzes a previously unpublished subset of data collected during an extensive wind tunnel campaign, the Unsteady Aerodynamic Experiment (UAE). The experimental data includes resultant flow fields, aerodynamic blade forces, and blade root flapwise bending moments all for both upwind and downwind configurations and, importantly, for the downwind one with an aerodynamic tower fairing. At high tip speed ratios (near design conditions), it is found in this paper that the tower shadow is a dominating contributor to bending moment oscillations but these can be mitigated by the use of a tower fairing when such a fairing is aligned with the flow.

I. Introduction

A. Downwind Rotors

An average wind turbine in 1980 had a 15 m rotor diameter and produced 55 kW of power (Quarton & Hanssan, 1998; Shikha & Kothari, 2003). Today, MHI Vestas manufactures turbines with a rotor diameter of 164 m with a world-record 8-9 MW rated power. Furthermore, Sandia National Laboratories (SNL) (Griffith & Ashwill, 2011) released the design for 'the hundred meter blade', and DTU Wind Energy Bak *et. al.*, 2012) has published work on a 10 MW reference turbine. However, the trend of increasing size is not as fast as in previous decades due to the increasing blade mass to accommodate stress levels that occur as the blades grow in length (Kim, Larsen & Yde, 2014). Structural limits are being reached with the conventional three-bladed, horizontal axis, upwind rotor design resulting in a search for innovative designs Veers, *et al.*, 2003). One option, especially being considered to reduce rotor mass is the use of a two-bladed downwind configuration. The first megawatt-scale wind turbine, Smith-Putnam turbine, used this configuration (Nielsen, 2010). Moving from an upwind rotor to a downwind rotor may give significant structural advantages, that can help support the evolution of extreme-scale wind turbines of 10-20 MW. (Loth, *et al.*, 2012; Icther, *et al.*, 2015)

However, a well-known concern with downwind turbines is the potential impact of tower shadow, i.e., the downstream wake from the tower impacting the blades as they pass through. The tower shadow is an aerodynamically unsteady region, with significant variations in flow angle and velocity, and with a net momentum deficit. As the downwind turbine blades pass through this region of velocity deficit and increased turbulence, the flow seen by the blade is directly modified. In particular, this can cause a rapid change of the blade's aerodynamic loading (Leishman, 2002; Zahle, *et al.*, 2009). The load fluctuations can increase fatigue damage, or excite a blade vibrational mode, increasing fatigue damage (Yoshida, Kiyoki, 2007). In addition to load fluctuation, tower shadow causes a distinct low frequency acoustic noise (Madsen, Aagaard, 2010). This tower shadow induced 'thumping' is the primary reason why upwind rotors became conventional over downwind (Koh, Ng, 2016).

Aerodynamic fairings to cover the tower have been a proposed solution to the tower shadow problem. More validation is required for the tower fairing solution, specifically the effectiveness of the fairing at

[1] Graduate Researcher, Mechanical and Aerospace Engineering.
[2] Research Scientist, Mechanical and Aerospace Engineering.
[3] Professor, Mechanical and Aerospace Engineering. Fellow AIAA

misaligned conditions (with non-zero fairing angle of attack), which can occur because of wind direction changes in environmental conditions (O'Connor, Loth & Selig, 2013).

B. Tower Shadow Experiments

To quantify and understand tower shadow, previous experimental studies (Orlando, *et al.* 2011) conducted an experiment to measure the wake caused by turbine towers at different Reynolds numbers. Anemometers were used to measure average wind speed at various locations. The experiment provided valuable understanding on the time averaged velocity deficit, as well as indicating the limitations of data measured with anemometers. However, the instrumentation only allowed for average data to be collected, which gives no insight into the instantaneous and unsteady structures of the wake and the data was collected from a tower without a rotor, which ignores any induction effect the rotor has on the wake flow field and does not allow direct examination of the impact on blade root moment.

Water tunnel experiments (O'Connor *et al*. 2013) experimentally investigated the wake behind a cylinder and thick symmetric airfoils at various angles of attack (0°, 10° & 20°) to mimic the wake behind a tower (faired and unfaired) at various yaw angles. They used Particle Image Velocimetry (PIV), to achieve a series of instantaneous realizations of the velocity field of the wake. This experiment provides an understanding of the effectiveness of fairings as a method of wake reduction at various yaw angles. However, as with the Orlando *et al.* study, no direct information was obtained on how the wake affects the rotor, and conversely no information is offered on how the rotor affects the wake.

The National Renewable Energy Laboratory (NREL) performed an experimental campaign Phase VI on the UAE turbine in the NASA Ames wind tunnel (Hand, *et al.*, 2001). Tests were conducted in both the upwind and downwind (faired and unfaired) configurations, as shown in Fig. 1. Instantaneous measurements were taken in full rotor operating conditions, leading to a better understanding of tower wake effects on the rotor blades, compared to previous experiments. Pressure taps at various positions along the blade provide a measure of aerodynamic load and consequently insight on tower shadow affects those loads. Strain gauges placed at the root of the blade, provide a measure of root bending loads. The tower shadow can be seen in Fig. 1a, by the flow visualization disturbed behind the tower. The tower fairing used in the experiment can be seen in Fig. 1b. This is perhaps the only data set to comprehensively and quantitatively examine the unsteady influence of the tower wake and that of fairings on flow fields, blade forces and moments (and such aspects have not been previously published).

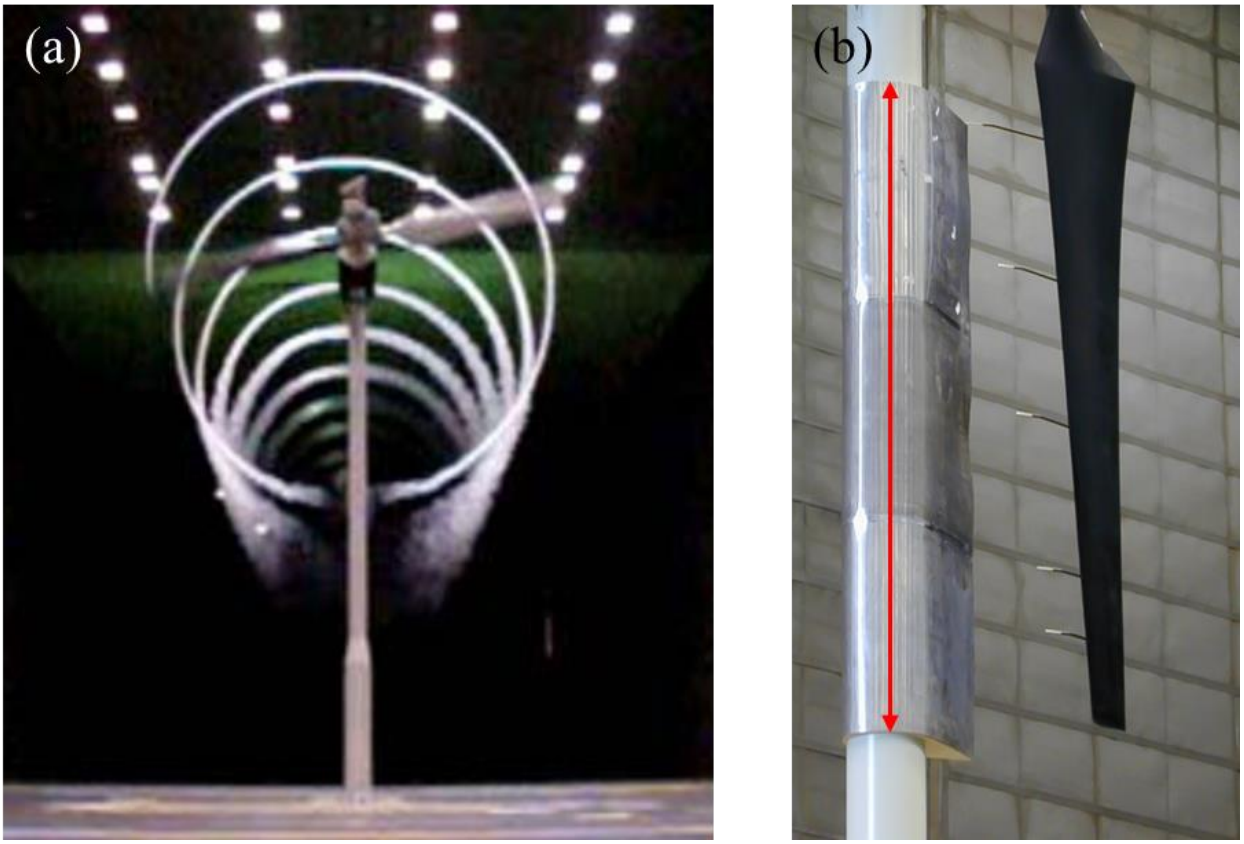

Fig. 1 UAE experimental configuration in the NASA Ames tunnel: (a) flow visualization of tip vortices, and (b) UAE tower fairing (with arrow indicating vertical extent) upstream of a UAE blade instrumented with 5-hole pressure probes

C. Objective

The present study has two primary objectives: 1) to analyze the effect of tower shadow on the blade flow condition as well as blade forces and moments for a downwind configuration, and 2) to assess the capability of a tower fairing to minimize this effect. To achieve these objectives, this study analyzes previously unpublished portions of a UAE experimental campaign, specifically those pertaining to downwind cases with a tower fairing both aligned and misaligned with the flow. This experimental campaign was unique in that it includes both the flow field measurement of the wake (important to understand wake physics), coupled with direct measurements of blade bending moments (important to understanding of resultant blade stress and fatigue). The present study is the first to analyze these fully-coupled unsteady shadow effects on a downwind turbine for various configurations and to compare these to a conventional upwind configuration. Using this unique data set can also allow insight into conditions when the tower shadow is likely to substantially influence blade bending moments, and the conditions for which a tower fairing may be useful in mitigating the negative effects of the tower shadow.

II. Experiment and Analysis

The Unsteady Aerodynamic Experiment (UAE) Phase VI (Hand, *et al.* 2001) was performed by NREL, at the NASA Ames Research Center, in the NFAC 80 ft x 120 ft test section, with less than 2% blockage. Several different turbine configurations were tested including, both upwind and downwind rotor configurations, both rigid and teetered rotors, both cylindrical and faired tower geometries. The test also included a variety of cone angles, yaw angles, blade pitch angles, rotor speeds, and tunnel inlet velocities. The general turbine parameters for the analyzed cases are outlined in Table 1. Measurements included flow pressure, flow angles, blade surface pressures, and blade loads at a rate of 520.83 (Hz). This study focuses

on the results that directly pertain to the differences between upwind and downwind rotors and those with and without the use of a tower fairing.

Table 1 General turbine parameters.

Blade Length	5.029 m
Hub Height	11.5 m
Tower Diameter	0.406 m
Rotational Speed	72 rpm
Shaft Tilt Angle	0°
Blade Pitch	3°
Rotor Yaw	0°

The objective of this study is to specifically investigate how the tower shadow affects the flow field seen by the blade, blade aerodynamic response, and the blade loading in terms of flapwise bending moment. For this, four different configurations were analyzed as shown in Fig. 2 and outlined in Table 2 based on three sequences:

1) From sequence H: an upwind rotor with a cylindrical tower (UC)
2) From sequence B: a downwind rotor with a cylindrical tower (DC)
3) From sequence 7: a downwind rotor with a tower fairing aligned with the flow (DF0)
4) From sequence 7: a downwind rotor with a tower fairing a misalignment angle, $\chi_F = 20°$ (DF20)

These four different configurations are shown in Fig. 2 and outlined in Table 2.

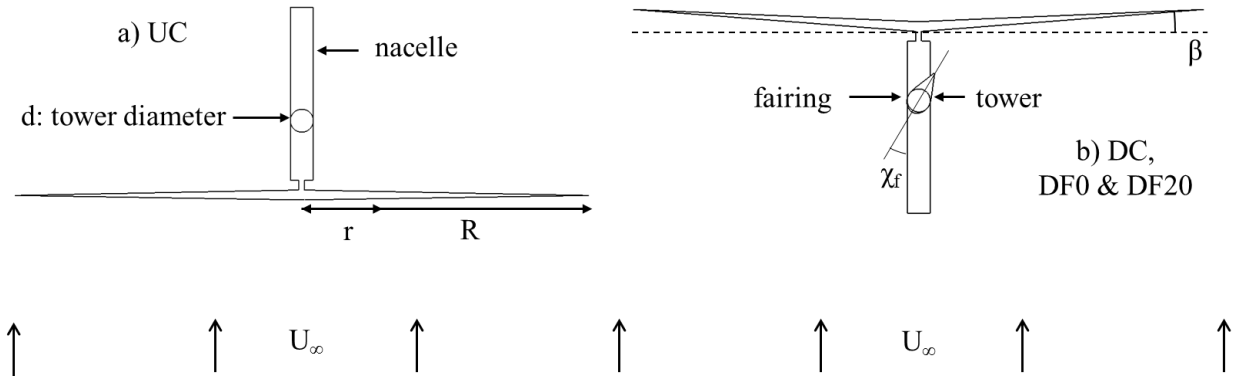

Fig. 2 Top view turbine schematic: (a) upwind rotor and (b) downwind rotor with fairing free to rotate about tower

Table 2 Case specific parameters.

	UC	DC	DF0	DF20
Cone Angle	0°	3.4°	3.4°	3.4°
Rigid/Teetered	Rigid	Teetered	Rigid	Rigid
Fairing Chord	NA	NA	0.89 m	0.89 m
Fairing Angle	NA	NA	0°	20°

Tests for all four configurations were completed at mean upstream velocities (U_∞) of 5, 7, 10, 15, 20 and 25 m/s. As this velocity approaches the rotor plane, it is slowed and modified by induction and other

effects, including any instantaneous wind deflection to tower wake for a downstream rotor configuration. The instantaneous wind velocity just upstream of the rotor is then defined as U, as shown in Fig. 3. The resultant flow vector seen by the blade at a given radius (r) is the combination of streamwise flow (U) and local blade rotational speed (ωr). The resultant velocity is defined by the resultant flow speed (V_r) and aerodynamic angle of attack (α) relative to the blade chord line. It should be noted that U and α as well as the flow details around the tower were not obtained directly in the UAE test but are related to other measurements that were obtained.

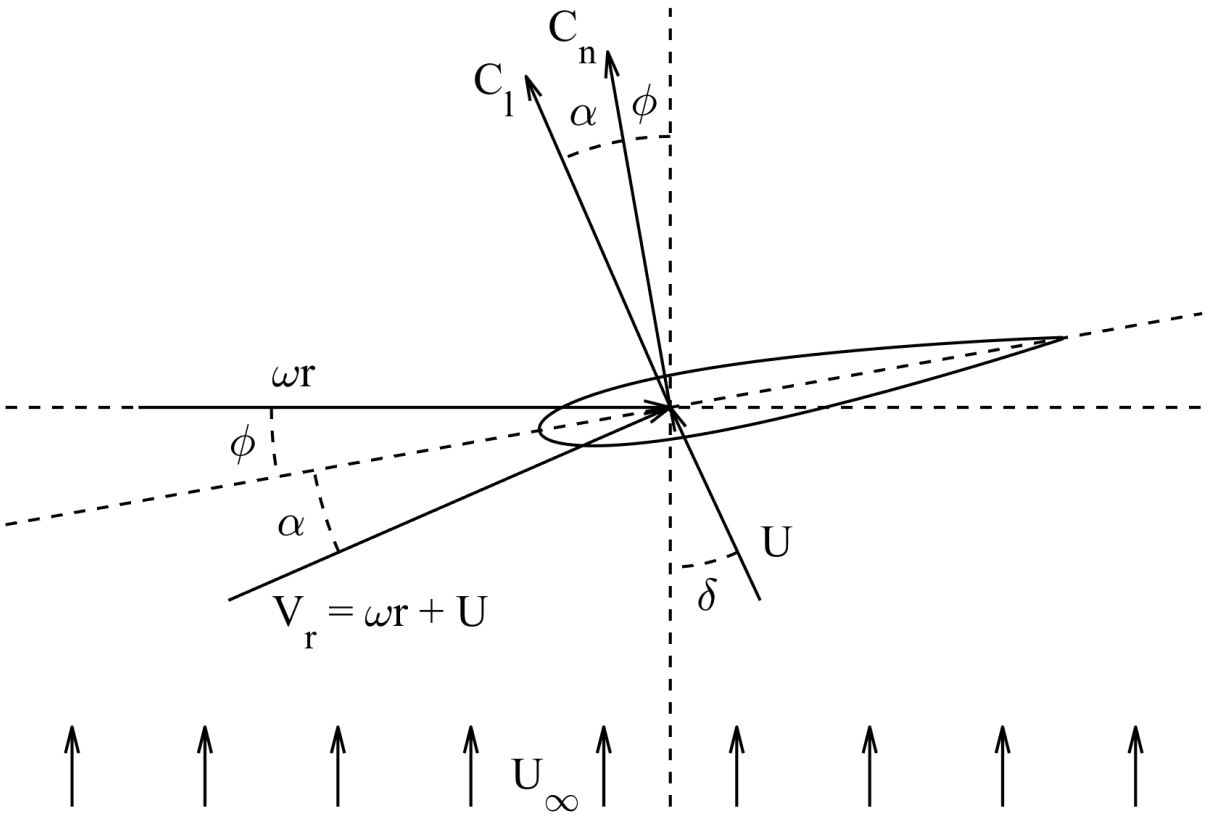

Fig. 3 Schematic of flow parameters: pitch plus local twist (ϕ), instantaneous wind deflection (δ), instantaneous wind (U), free stream wind (U_∞), angle of attack (α), rotational velocity (ωr), where C_n is normal to chord line & C_l is normal to the resultant flow (V_r).

In particular, four of the measured variables from the test were analyzed herein: Local flow angle (LFA), resultant velocity (V_r), normal force coefficient (C_n), and root flapwise bending moment (M). The flow parameters were measured at r/R = 0.34, 0.51, 0.67, 0.84 & 0.91 with 5-hole probes extending ahead of the blade by 80% the local chord length (Hand, *et al.*, 2001). Importantly, LFA values based on these probes are related to, but differ from, α. The differences are described later in the Results and Discussion section. Surface pressures were also measured along the blade surface using pressure taps, which were then used to calculate pressure coefficient at various positions along the span and chord. Integrating these pressure coefficients along the chord at r/R = 0.30, 0.47, 0.63, 0.80 & 0.95 (and neglecting skin friction effects) yielded the local aerodynamic normal force coefficient (C_n). Local blade properties at two of the key spanwise stations are provided in Table 3. Finally, strain gauges mounted at the blade root were used to measure M.

Table 3 Geometric properties at key spanwise locations.

r/R	Chord Length (m)	Pitch + Twist (degrees)	Rotational Speed (m/s)
0.63	0.543	4.150	23.9
0.67	0.523	3.719	25.4

III. Results and Discussion

The results are examined in the order of causation influence, starting with the tower shadow impact on flow angles and flow speeds seen by the blades, followed by examining how these speeds an angles impact the aerodynamic blade forces, and the blade root bending moments. The tip speed ratio (TSR) is 5.42 at upstream velocity (U_∞) of 7 m/s. This TSR is a typical magnitude for many turbines. For example, the NREL 5MW reference turbine has a TSR of 7.08 at rated conditions. The highest TSR case (U_∞ = 5 m/s) was not chosen for in depth analysis because the lower inlet speed lead to relatively high turbulence in the wind tunnel and therefore a high signal to noise ratio. For this reason, the cases at U_∞ = 7 m/s are analyzed in the most depth. The tower Reynolds number at U_∞ = 7 m/s based on tower diameter is 189,000, which is in the super-critical drag regime.

A. Effect on Resultant Flow Field

The 5-hole pressure probes used in the UAE experiment measured the local flow field at 0.8 chord length in front of the airfoil (Hand, *et al.*, 2001). The local flow angle (LFA) is generally not equal to the local aerodynamic angle of attack (α, of Fig. 3) since the LFA also includes effects associated with the local aerodynamic influence of the blade on the flow just upstream, including effects of a) upwash due to local lift, b) streamline deviation due to blade finite thickness, c) swirl induced by the rotor, and d) tip vortices. The differences between LFA and α for the UAE have been investigated in depth (Sant *et al.* 2006) but an accurate relationship that can be used as a general theoretical correction was not found. Since no relationship is available, it is only noted herein that LFA is related to, but not equal to, α. Figure 4 shows the LFA at r/R=0.67 for 36 complete revolutions. This radial location was chosen as the point that approximately separates the swept area in half, i.e. the area inboard of this location approximately equals the swept area outboard of the location. For the upwind case (UC), the LFA is smooth and generally unaffected by the tower shadow, this is in part due to the large overhang for the rotor. Conversely, in all three downwind cases the LFA is greatly influenced by the tower shadow. This is especially true in the region of $160° < \psi < 200°$, where the LFA varies significantly. In particular, there is a strong average decrease (black line) in LFA near $\psi \sim 180°$. In the region, the instantaneous data (gray points) varies significantly from the average. This is due to the rotor passing through an unsteady wake with positive and negative wind deflection (δ from Fig. 3).

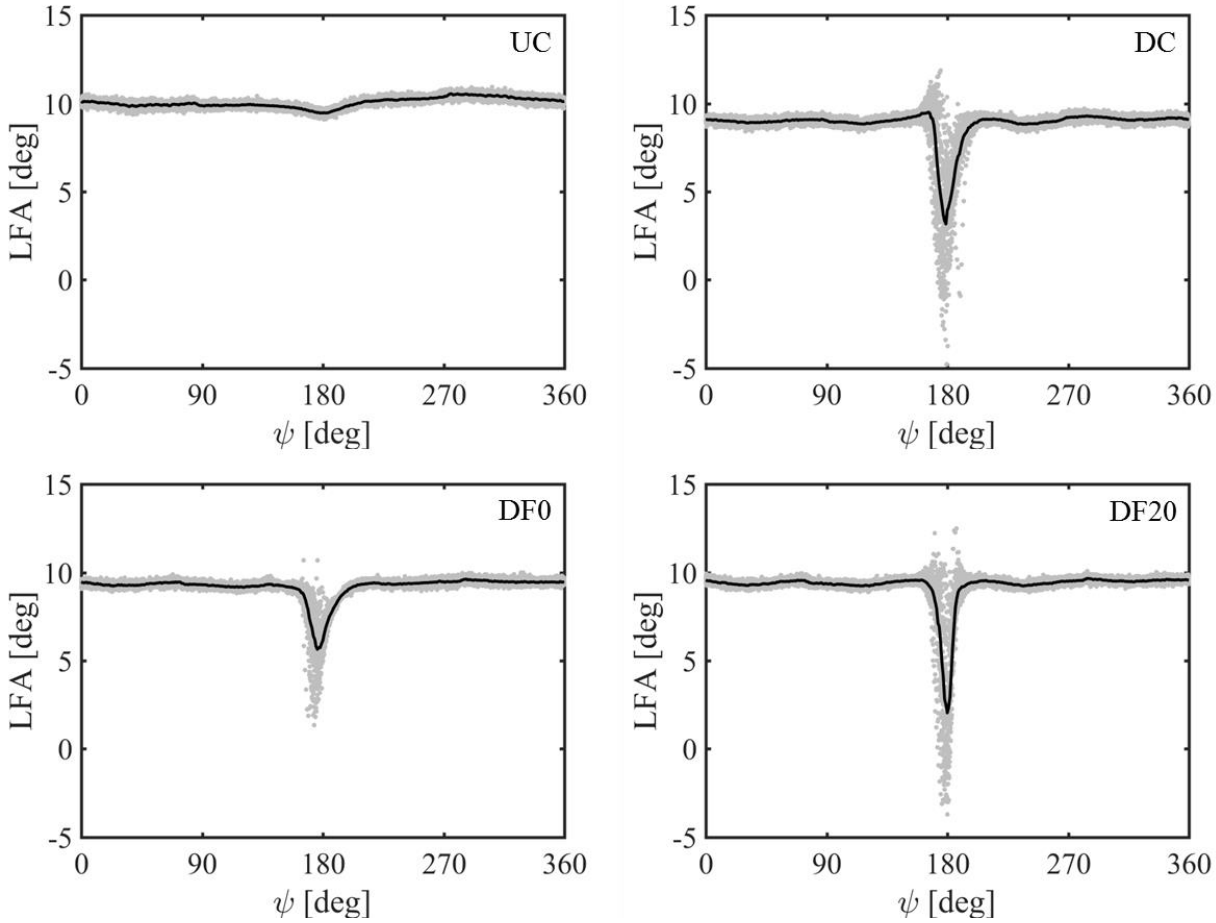

Fig. 4 Local flow angle as function of azimuthal angle at r/R=0.67 and U_∞=7m/s. The grey dots indicate instantaneous measured values while the solid black line indicates the cycle-averaged measurements (averaging all values for a given ψ value).

An interesting phenomenon observed is that LFA is not symmetric about ψ=180°, primarily in the DC case. Near ψ~170°, the instantaneous values of LFA can be significantly higher than wake-free values (ψ<160° & ψ>200°). This increase is not seen as the blade exits the wake (ψ~190°) demonstrating that the tower shadow effect is not simply a symmetric reduction in LFA. Since this asymmetry occurs upstream of the blade, it is likely due an interaction effect between rotor swirl and the tower wake. Such an upstream influence causing asymmetry was previously suggested by Zahle *et al*. (Zahle, *et al.*, 2009) Another indication of slight azimuthal asymmetry is that the drop in average LFA entering the wake is steep whereas the return to wake-free values is relatively slower. When comparing the downwind cases of a cylinder tower (DC) vs. a faired tower (DF0), there is an interesting difference in instantaneous extremes. The DC case has LFA values as low as -5° and as high as 12°, whereas the DF0 LFA values are generally confined between 0° and 10°. In general, the DF0 case has variations are limited to be about one-half that of the DC case. However when the misalignment angle, χ_F, is increased to 20° in the DF20 case, LFA seen by the blade for the faired tower is similar to the un-faired case. This suggests that the fairing alignment angle is critical to mitigate tower shadow effects.

If one considers the cycle-averaged experimental data for the DC case (solid black line), there is a noticeable wake asymmetry seen in the LFA deficit, whereby the drop in LFA entering to the wake is quicker than the subsequent LFA recovery exiting the wake. This asymmetry can be attributed to a coupled effect of the rotor interacting with vortexes from the wake (Zahle *et al*, 2009).

Figure 5 shows the resultant velocity (V_r), taken at r/R=0.67, plotted against azimuth angle. As expected, there is little variation with azimuth angle in the upwind case, but there is a significant shadow effect in the downwind cases. The average V_r is affected by the tower shadow in all three downwind configurations, although the trend is not consistent. As the blade passes through the wake, there is a slight increase in average flow speed for DC & DF0, but a decrease for DF20. This is not easily explained. Perhaps the fairing turned the flow slightly into the oncoming rotor, which increased the relative flow speed for DF0. Of larger significance are the instantaneous deviations from the average. The deviations are of a magnitude of ±4m/s for DC, ±2m/s for DF0 and ±3m/s for DF20. These significant variations are attributed to the fact that the wake from a cylinder (or fairing) can cause the flow to deflect into and away from (as a function of time) the oncoming rotor. As shown in Fig 3, δ ranging from large positive to large negative values will change the magnitude of V_r.

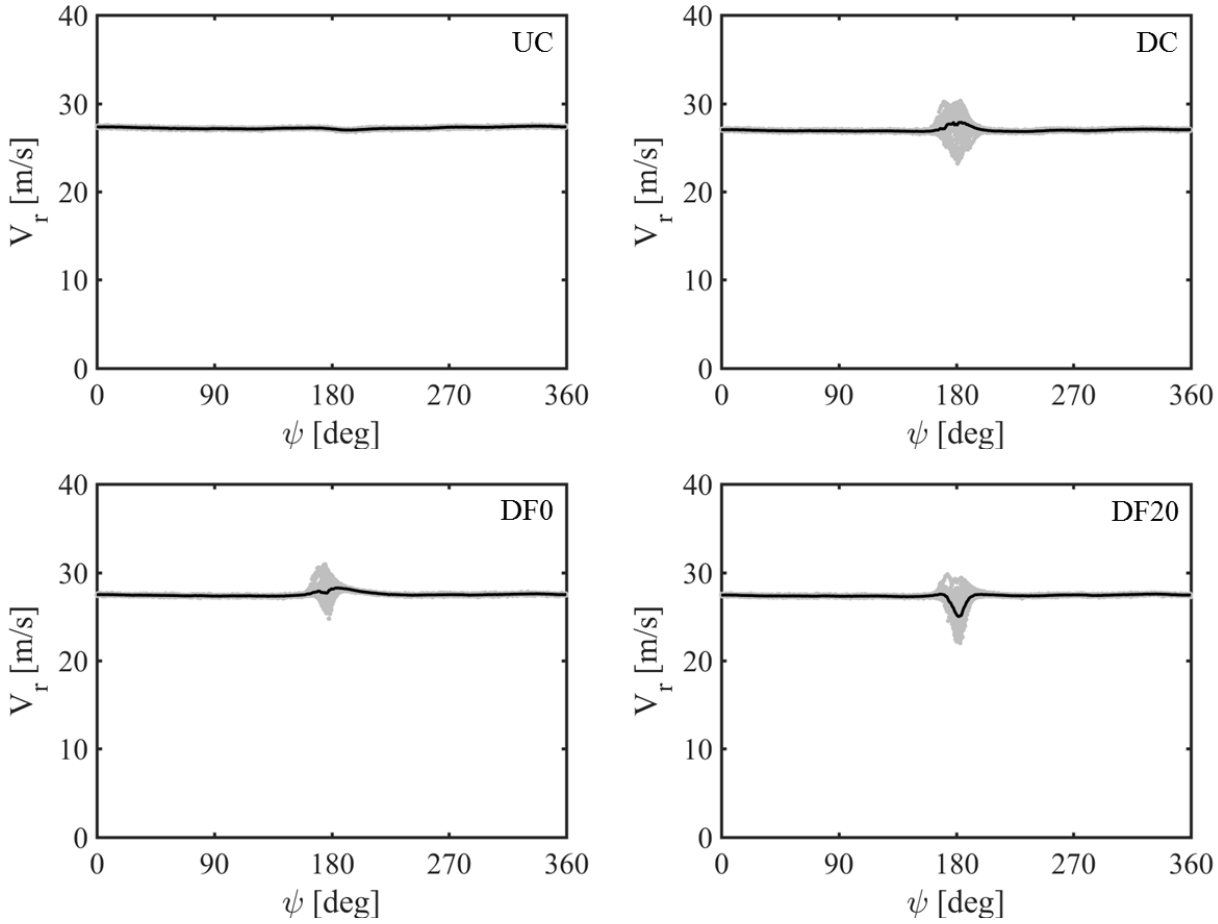

Fig. 5 Resultant velocity as function of azimuthal angle at r/R=0.67 and U_∞=7m/s using same symbol representation as in Fig. 4.

B. Effect on Aerodynamic Loads

Figure 6 shows the normal force coefficient, taken at r/R=0.63, plotted against azimuth angle. With respect to the shadow effects in the experimental data, the plots of C_n have many of the same qualitative characteristics as the plots from the LFA (Fig. 4), i.e. a pronounced dip and wake asymmetry. The tower shadow does not only lead to a force reduction. There are instantaneous cases where the loads are significantly larger inside the tower shadow than the wake free values. Primarily as a result of the flow angle effects, the fairing decreases the peak C_n deficit in the DF0 case by about two-fold. Again, this

reduction is lost for the DF20 (misaligned fairing) case as it behaves similarly to the DC (cylindrical tower case).

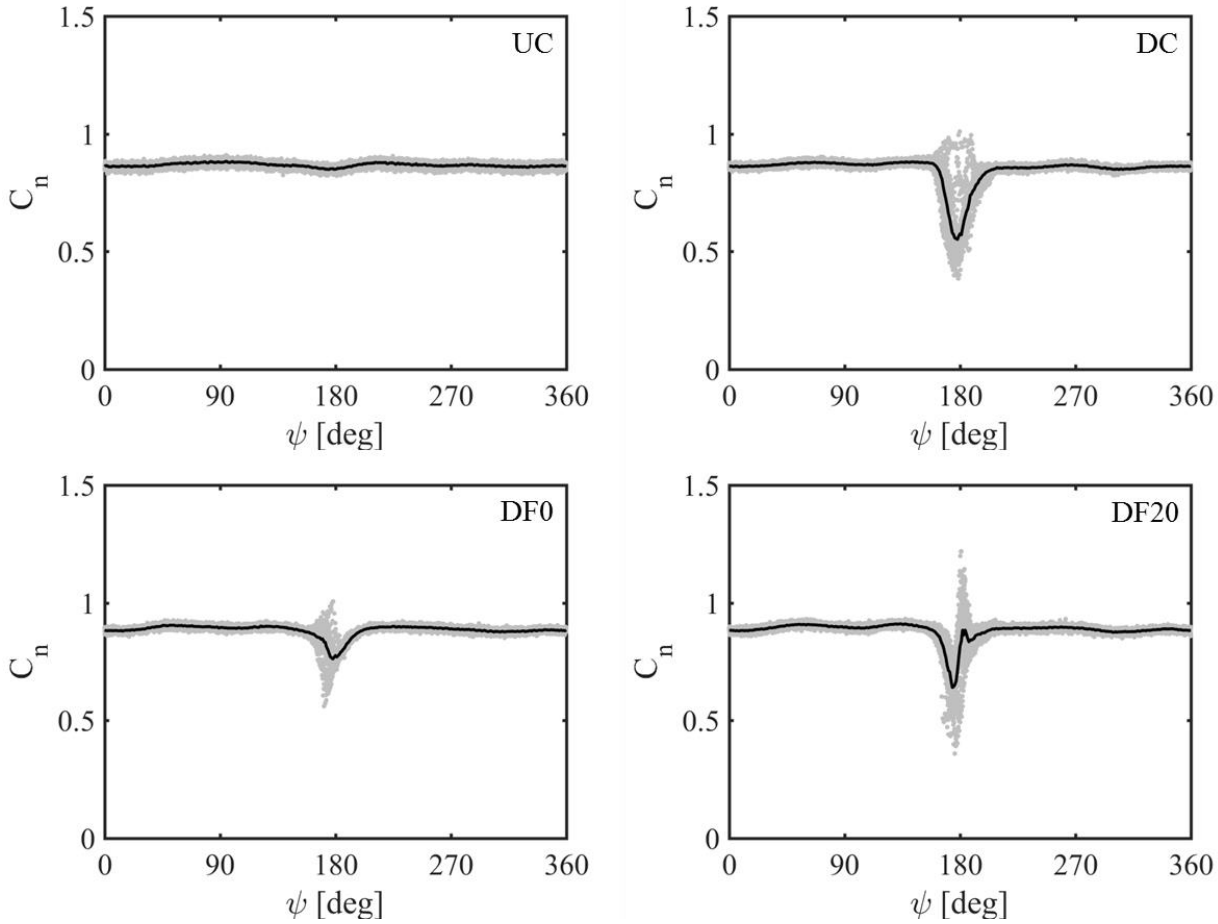

Fig. 6 Normal force coefficient as function of azimuthal angle at r/R=0.63 and U_∞=7 m/s using same symbol representation as in Fig. 4.

C. Effect on Blade Bending

Figure 7 shows root flap bending moment plotted against azimuth angle. There is an average offset between the upwind and downwind cases, of about 1 kN·m. This offset is attributed to the differences in the relative coning angle for the rotors. In particular, the upwind rotor has no coning but the downwind rotors have a downwind coning of 3.4°. This coning leads to a negative M, due to centrifugal loading countering the positive thrust loads. All the downwind cases show oscillation in the moment at a rate of 6/rev, which is attributed to the natural structural frequency associated with flapwise stiffness of the blade being excited by the tower shadow.

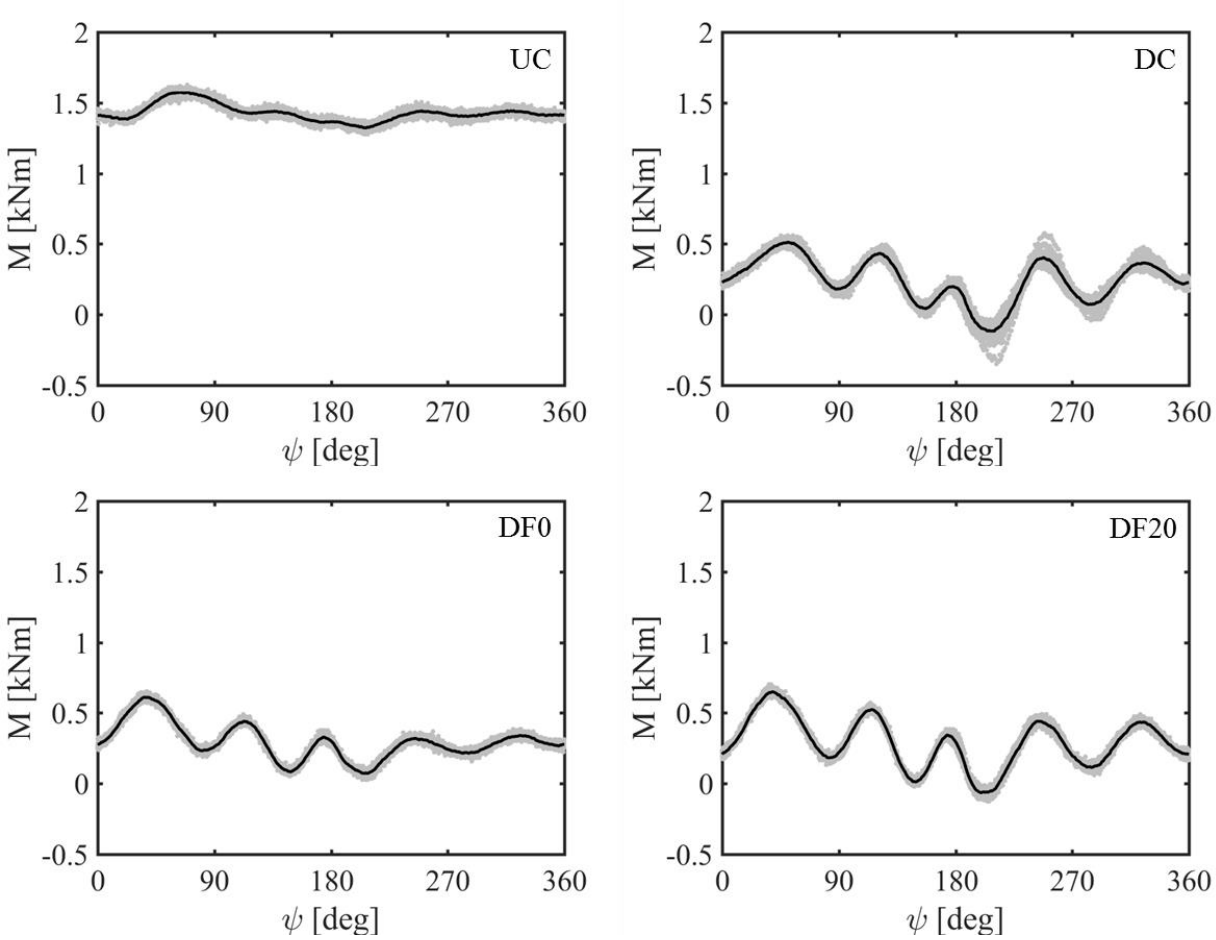

Fig. 7 Root flap bending moment as function of azimuthal angle at U_∞ = 7 m/s using same symbol representation as in Fig. 4.

It is quite interesting that the tower shadow effect for M (which is integrated over the blade span and depends more strongly on blade dynamics and aero elasticity) differs substantially from the effect LFA, V_r and C_n previously analyzed (which are primarily associated with local flow features). For the bending moment of the downwind cases, there is no sharp drop in bending load centered at ψ~180°. Instead, the shadow effect appears to be an impulse (with a negative sign) at ψ=180°, resulting in under-damped oscillations. For the DC case, the magnitude of the oscillations is increased by about four-fold compared with the UC case, indicating that the tower shadow effect can substantially increase blade bending loads and therefore the potential for fatigue failure. The fairing reduces the magnitude of the fluctuations by about 50%, whereas the DF20 case shows no improvement over the (unfaired) cylindrical (DC) case.

IV. Conclusions

The first objective of this study was to investigate the effects of tower shadow on the flow seen by the blade as well as the blade forces and moments. At low freestream velocities (high tip speed ratios), there was a pronounced tower shadow effect on the resultant flow angle deficit and fluctuations but a relatively weak influence on resultant velocity magnitude seen by the blade. This flow angle effects translated to distinct effects on the normal force coefficient, and blade bending moments. The second objective focused on the effectiveness of tower fairing to mitigate the tower shadow effect. The flow-aligned fairing reduced the tower shadow effects on the resultant flow field, leading to a reduced effect on the normal force coefficient. However, the faring misaligned with the flow by 20° did not reduce shadow effect in any significant way. As such, fairing concept can be considered an option to mitigate tower shower effects, but

that its benefits may be eliminated if the flow is misaligned by about 20 degrees. Recommended future experimental work includes investigating the tower shadow effects for a downwind rotor in field conditions with cylindrical tower and for a lightweight self-aligning fairing, to determine if this can allow a net positive mitigation of the shadow effects.

Acknowledgements

The authors would like to thank NREL for their support and guidance through the project. Specifically the authors would like to thank Scott Schreck and Patrick Moriarty, who gave of their time and energy repeatedly to advise the project.

REFERENCES

1. Quarton, D. C. "The evolution of wind turbine design analysis—a twenty year progress review." *Wind Energy* 1.S1 (1998): 5-24.
2. Shikha, Bhatti, T., & Kothari, D. (2003). Aspects of Technological Development of Wind Turbines. *Journal of Energy Engineering*, *129*(3), 81–95. https://doi.org/10.1061/(ASCE)0733-9402(2003)129:3(81)
3. Griffith, D. Todd, and Thomas D. Ashwill. "The Sandia 100-meter all-glass baseline wind turbine blade: SNL100-00." *Sandia National Laboratories, Albuquerque, Report No. SAND2011-3779* (2011).
4. Bak, Christian, et al. "Light Rotor: The 10-MW reference wind turbine." *EWEA 2012-European Wind Energy Conference & Exhibition*. 2012.
5. Kim, Taeseong, Torben J. Larsen, and Anders Yde. "Investigation of potential extreme load reduction for a two-bladed upwind turbine with partial pitch." *Wind Energy* 18.8 (2015): 1403-1419.
6. Veers, Paul S., et al. "Trends in the design, manufacture and evaluation of wind turbine blades." *Wind Energy* 6.3 (2003): 245-259.
7. Nielsen, Kristian H. "Technological trajectories in the making: two case studies from the contemporary history of wind power." *Centaurus* 52.3 (2010): 175-205.
8. Loth, Eric, et al. "Segmented ultralight pre-aligned rotor for extreme-scale wind turbines." *50th AIAA Aerospace Sciences Meeting including the New Horizons Forum and Aerospace Exposition*. Nashville, Tennessee: AIAA, 2012.
9. Ichter, Brian, et al. "A morphing downwind-aligned rotor concept based on a 13-MW wind turbine." *Wind Energy* 19.4 (2016): 625-637.
10. Leishman, J. Gordon. "Challenges in modelling the unsteady aerodynamics of wind turbines." *Wind energy* 5.2-3 (2002): 85-132.
11. Zahle, Frederik, Helge Aagaard Madsen, and Niels N. Sørensen. "Evaluation of tower shadow effects on various wind turbine concepts." *Risoe*. Danmarks Tekniske Universitet, Risø Nationallaboratoriet for Bæredygtig Energi, 2009. 11-29.
12. Yoshida, Shigeo, and Soichiro Kiyoki. "Load equivalent tower shadow modeling for downwind turbines." *Nippon Kikai Gakkai Ronbunshu B Hen(Transactions of the Japan Society of Mechanical Engineers Part B)(Japan)* 19.6 (2007): 1273-1279.
13. Madsen, Helge Aagaard. "Low frequency noise from wind turbines mechanisms of generation and its modelling." *Journal of Low Frequency Noise, Vibration and Active Control* 29.4 (2010): 239-251.
14. Koh, J. H., and E. Y. K. Ng. "Downwind offshore wind turbines: Opportunities, trends and technical challenges." *Renewable and Sustainable Energy Reviews* 54 (2016): 797-808.
15. O'Connor, Kyle, Eric Loth, and Michael S. Selig. "Design of a 2-D fairing for a wind turbine tower." *31st AIAA Applied Aerodynamics Conference*. 2013.
16. Orlando, Stephen, Adam Bale, and David A. Johnson. "Experimental study of the effect of tower shadow on anemometer readings." *Journal of Wind Engineering and Industrial Aerodynamics* 99.1 (2011): 1-6.
17. Hand, M. M., et al. *Unsteady aerodynamics experiment phase VI: wind tunnel test configurations and available data campaigns*. No. NREL/TP-500-29955. National Renewable Energy Lab., Golden, CO.(US), 2001.
18. Zahle, Frederik, Niels N. Sørensen, and Jeppe Johansen. "Wind turbine rotor-tower interaction using an incompressible overset grid method." *Wind Energy* 12.6 (2009): 594-619.
19. Sant, Tonio, Gijs van Kuik, and G. J. W. Van Bussel. "Estimating the angle of attack from blade pressure measurements on the NREL phase VI rotor using a free wake vortex model: axial conditions." *Wind Energy* 9.6 (2006): 549-577.